

## **PRECRACKED RC T-BEAMS REPAIRED IN SHEAR WITH BONDED CFRP SHEETS**

Samir Dirar, Janet Lees and Chris Morley

**Samir Dirar** is a Lecturer in Structural Engineering at the University of Birmingham, United Kingdom (UK). He received his PhD in Engineering from the University of Cambridge, UK. His research interests include strengthening of existing structures with fiber reinforced polymers, nonlinear finite element analysis of concrete structures and structural health monitoring.

**Janet Lees** is a Senior Lecturer in Structural Engineering at Cambridge University, UK. She is interested in the use of advanced durable materials as prestressing tendons for concrete elements, strengthening and repair of existing structures, advanced numerical analyses, glass fiber reinforced polymer pipelines and sustainable concrete.

**Chris Morley** is a former Senior Lecturer in Concrete Structures at Cambridge University, UK. He has always been interested in plasticity theory, and especially in its application to reinforced concrete (RC) structures. His research interests extend to nonlinear finite elements analysis of RC structures, water in hardened concrete and structural analysis generally.

### **ABSTRACT**

This paper investigates the structural behavior of precracked reinforced concrete (RC) T-beams strengthened in shear with externally bonded carbon fiber reinforced polymer (CFRP) sheets. It reports on seven tests on unstrengthened and strengthened RC T-beams identifying the influence of load history, beam depth and percentage of longitudinal steel reinforcement on the structural behavior. The experimental results indicate that the contributions of the external CFRP sheets to the shear force capacity can be significant and depend on most of the investigated variables.

This paper also investigates the accuracy of the prediction of the FRP contribution in ACI 440.2R-08; UK Concrete Society TR 55 and *fib* Bulletin 14 design guidelines for shear strengthening. Comparison of predicted values with experimental results indicates that the guidelines can overestimate the shear contribution of the externally bonded fiber reinforced polymer (FRP) system.

**Keywords:** beam; fiber reinforced polymer; precracking; reinforced concrete; shear; strengthening

## INTRODUCTION

Throughout the world many existing reinforced concrete (RC) structures are deemed no longer able to sustain current capacity demands. In the United Kingdom (UK) alone, it has been estimated that there are about 10,000 bridges on the motorway and trunk road network (the majority of which are reinforced and prestressed concrete structures) and 150,000 bridges on local roads of which a considerable number need strengthening or replacement<sup>1</sup>. The estimated cost of assessing and strengthening these strength-deficient structures is in excess of £4 billion<sup>2</sup>. Other countries are faced by the same problem. In the United States (US) for example, of the 600,905 bridges across the country, 72,868 bridges (12.1%) were categorized as structurally deficient and 89,024 bridges (14.8%) were categorized as functionally obsolete. The estimated cost of strengthening and repairing both categories is about US\$140 billion<sup>3</sup>.

Several factors can cause a RC structure to be judged as having insufficient capacity. The need to sustain heavier loads is one important factor, particularly in the case of bridges. Further factors that can have detrimental effects on capacity include corrosion of internal steel reinforcement, changes in use, poor initial design and more stringent assessment codes. One viable solution is to use fiber reinforced polymers (FRPs) as external strengthening reinforcement for RC structures. The use of FRPs is advantageous since the combination of high-strength, high-stiffness structural fibers with low-cost, lightweight, environmentally resistant polymers results in composite materials with excellent mechanical and durability properties.

During the past two decades, several research studies have considered RC beams strengthened in shear with externally bonded FRP systems. However, there are areas where further research is still needed. T-beams have not been considered as extensively as rectangular beams and in general studies investigating the effect of load history on the strengthened behavior have been scarce. Therefore, an attempt is made in this paper to investigate the effect of load history on the behavior of precracked RC T-beams strengthened in shear with carbon FRP (CFRP) sheets. Other parameters that may influence behavior, namely the effective depth of the beam and the longitudinal steel reinforcement ratio, are also discussed. Finally, the reliability of the prediction of the FRP shear contribution in three international shear strengthening design guidelines, namely ACI 440.2R-08<sup>4</sup>; UK Concrete Society TR 55<sup>5</sup> and *fib* Bulletin 14<sup>6</sup>, is examined.

## RESEARCH SIGNIFICANCE

Many researchers<sup>e.g. 7-11</sup> have investigated the technique of strengthening RC beams in shear using FRPs and established its effectiveness. Published research studies have provided valuable findings, particularly with regard to the effects of the type, stiffness and configuration of the composite material on the shear strength enhancement. However, other parameters that may also influence the shear resisting mechanisms, such as the load history, have not yet been sufficiently studied. In addition to investigating the effect of load history on the shear strength enhancement, this study simulates aspects of the in-service behavior of FRP-strengthened beams including precracking and strengthening under load.

## EXPERIMENTAL INVESTIGATION

The experimental investigation consisted of two unstrengthened control beams along with five other beams that were precracked prior to the application of the CFRP sheets. All specimens were T-shaped beams having a significant difference between their unstrengthened shear capacity and their flexural capacity. The T-shaped cross-section was favored because it adequately simulates the slab-on-beam construction method. The gap between the shear capacity and the flexural capacity was deemed necessary in order to provide a sufficient range over which the level of shear enhancement could be measured.

Each specimen had a four part designation given as  $X/d/LP\#/p$  where  $X$  indicates that the beam was either unstrengthened (U) or strengthened with CFRP fabrics (F),  $d$  is the effective depth of the beam in mm,  $LP\#$  indicates the loading pattern to which the beam was subjected and  $p$  indicates the longitudinal reinforcement ratio ( $A_s/b_w d$ ) of the beam. Hence, the designation F/295/LP1/4.5 refers to a beam that was strengthened with CFRP fabrics (sheets), had an effective depth of 295 mm (11.61 in.), tested under loading pattern 1 (LP1) and had a longitudinal reinforcement ratio of 4.5%.

All tested shear spans had 6 mm (0.24 in.) internal steel transverse reinforcement spaced at 250 mm (9.84 in.) c/c. For the strengthened beams, the external shear reinforcement on a strengthened shear span consisted of three layers of CFRP sheets.

The two T-shaped cross-sections considered in this experimental investigation are detailed in **Fig. 1**. Additional details of the test specimens are given in **Table 1**.

### Loading patterns

Three loading schemes were adopted for testing. Loading Pattern 0 (LP0), which was only applied to test the control specimen U/295/LP0/4.5, consisted of loading the beam up to

1 failure. The remaining two loading patterns, namely Loading Pattern 1 (LP1) and Loading  
2 Pattern 2 (LP2), involved the pre-cracking of the test specimens in order to model the state of  
3 damage that may exist in RC structures requiring strengthening. Tests on the unstrengthened  
4 beams showed that the state of damage caused by a load level of about 70% of the  
5 unstrengthened shear force capacity can be representative of the state of damage that may  
6 exist in some RC structures requiring strengthening. Hence, that load level was used in both  
7 LP1 and LP2 described below. Since RC structures may also be carrying dead loads while  
8 being strengthened, specimens were unloaded to a proportion of the unstrengthened capacity  
9 before the CFRP strengthening system was applied. The final phase involved loading the  
10 strengthened specimens up to failure.

11 Specimens subjected to LP1 were loaded, as shown in **Fig. 2**, to 70% of the unstrengthened  
12 capacity of the corresponding control beam. Specimens were then unloaded to 40% of the  
13 unstrengthened capacity of the corresponding control beam and the strengthening system was  
14 installed. Loading then continued up to failure. Under this loading pattern, the shear cracks  
15 formed prior to strengthening are likely to be mobilized once strengthened.

16 LP2 aims to stimulate a set of shear cracks after strengthening that are different from those  
17 formed prior to strengthening. Specimens subjected to LP2 were initially loaded at position  
18 (B), as illustrated in **Fig. 2**, to 70% of their unstrengthened capacity. Specimens were then  
19 unloaded to 40% of their unstrengthened capacity and the strengthening system was installed.  
20 Load was then shifted gradually to position (A) and continued up to the failure of the  
21 specimens. The total load was kept constant at 40% of the unstrengthened capacity of the test  
22 beam as it was shifted from position (B) to position (A).

23

#### 24 **Test setup**

25 All the beams except U/295/LP2/4.5 and F/295/LP2/4.5 represented a single specimen tested  
26 in four-point bending (see **Fig. 3**). However, in order to speed up the final stages of the  
27 testing process, U/295/LP2/4.5 and F/295/LP2/4.5 were tested in three-point bending as this  
28 type of loading allowed two tests to be carried out on a single beam. This was achieved by  
29 testing one beam end zone while keeping the other end overhung and unstressed and vice  
30 versa (see **Fig. 3**). The 925 mm (36.42 in.) long shear span was reinforced with additional  
31 transverse steel reinforcement (6 mm [0.24 in.] shear links spaced at 100 mm [3.94 in.] c/c) to  
32 ensure that failure always occurred in the 1125 mm (44.29 in.) long shear span. The shear  
33 span to effective depth ratio ( $a/d$ ) in all beams was maintained at a value of 3.8.

34

## 1 **Materials**

2 The concrete used to cast the specimens consisted of coarse gravel aggregate (10 mm [0.39  
3 in.] maximum size), fine aggregate (sand) and ordinary Portland cement (ASTM C150 Type  
4 D). The mix proportions by weight were cement : sand : gravel = 1 : 2.75 : 3.36. The  
5 water/cement ratio was 0.7. The targeted cube compressive strength after 28 days was 25  
6 MPa (3.63 ksi). This value was favored because it simulates the deterioration in the concrete  
7 compressive strength that may exist in deficient RC structures.

8 Tensile tests were carried out on the steel reinforcement used in this study in order to quantify  
9 its mechanical properties. The test results for the strength and stiffness properties of the steel  
10 reinforcement are given in **Table 2**.

11 The CFRP fabrics (sheets) used in this investigation were the commercially available  
12 SikaWrap-230C. These are unidirectional woven carbon fiber fabrics that are usually used in  
13 conjunction with an epoxy laminating resin, in this case Sikadur-330, to provide a composite  
14 strengthening system. The fabric, adhesive and laminate (i.e. fabric + adhesive) properties, as  
15 obtained from the manufacturer's data sheets<sup>12,13</sup>, are presented in **Table 3**.

16

## 17 **Instrumentation**

18 The deflections of all specimens were measured with linear resistance displacement  
19 transducers (LRDTs). The LRDTs were positioned either at mid-span for the beams tested in  
20 four-point bending or at position (A), i.e. at  $a = 3.8d$  (see **Fig. 2**), for the specimens tested in  
21 three-point bending.

22 The strain in the transverse steel reinforcement and in the CFRP sheets was measured with  
23 strain gauges. The strain gauges were bonded to the internal steel reinforcement before  
24 casting whereas the strain gauges on the CFRP sheets were bonded to the surface of the sheet  
25 after it had cured but before starting the final phases of LP1 and LP2. **Fig. 3** illustrates the  
26 locations of these strain gauges. The strain gauges on the transverse steel reinforcement are  
27 designated TR# where # indicates the strain gauge number. Similarly, CF# indicates the  
28 strain gauge number for the strain gauges on the CFRP sheets. Strain gauges on the steel and  
29 CFRP shear reinforcement are spaced 250 mm (9.84 in.) c/c.

30 The LRDTs and strain gauge readings were acquired using an automatic data logging system.

31

## 32 **EXPERIMENTAL RESULTS AND DISCUSSION**

### 33 **Shear force capacity**

1 The unstrengthened shear capacity of each specimen as well as the shear force at failure and  
2 the gain in shear capacity above the corresponding unstrengthened control beam are  
3 presented in **Table 4**. The unstrengthened control beam tested by Hoult and Lees<sup>14</sup> is  
4 nominally identical to F/215/LP1/4.6 and F/215/LP2/4.6. Hence, it will be used as a basis of  
5 comparison for these two beams. It failed in shear at a shear force of approximately 88 kN  
6 (19.78 kips).

7 Specimen U/295/LP0/4.5 was an unstrengthened control beam designed to fail in shear in  
8 order to create a baseline reading for the 350 mm (13.78 in.) deep specimens. The  
9 unstrengthened specimen U/295/LP2/4.5 was tested to examine the effect of LP2 on the shear  
10 carrying capacity of an unstrengthened beam.

11 The shear force carried by U/295/LP0/4.5 at failure was 107 kN (24.05 kips). The other  
12 unstrengthened specimen, i.e. U/295/LP2/4.5, attained a shear force of 116 kN (26.08 kips) at  
13 failure. The difference in shear force capacity between the two specimens was approximately  
14 8%, suggesting that using LP2 had little significant effect on the shear force capacity of  
15 U/295/LP2/4.5.

16 The 350 mm (13.78 in.) deep strengthened specimens F/295/LP1/4.5 and F/295/LP2/4.5  
17 failed at a shear force of 135 kN (30.35 kips) and 133.5 kN (30.01 kN) respectively, attaining  
18 increases in shear force capacity of 26.2% and 24.8% respectively. The corresponding 270  
19 mm (10.63 in.) deep strengthened specimens (F/215/LP1/4.6 and F/215/LP2/4.6) failed at a  
20 shear force of 102.5 kN (23.04 kips) and 96.5 kN (21.69 kips) respectively, achieving  
21 increases of 16.5% and 9.7% respectively.

22 Specimen F/295/LP1/3.3 attained a shear force of 122.5 kN (27.54 kips) at failure  
23 corresponding to 14.5% shear enhancement. This specimen failed in flexure. Although not  
24 reported in detail in this paper, the readings of strain gauges on the longitudinal steel of  
25 F/295/LP1/3.3 showed clearly that yielding had occurred. Due to the flexural failure of  
26 F/295/LP1/3.3, it is possible that the difference in the shear carrying capacities between  
27 F/295/LP1/3.3 and F/295/LP1/4.5 is a consequence of specimen F/295/LP1/3.3 attaining its  
28 flexural capacity rather than a consequence of the change in the longitudinal reinforcement  
29 ratio. Hence, it can only be concluded that the capacity of F/295/LP1/3.3 was increased by at  
30 least 15.5 kN (3.49 kips).

31 The two load histories investigated, LP1 and LP2, did not generally seem to have a  
32 significant effect on the load carrying capacity of the strengthened beams. There was less  
33 than a 7% capacity difference in the 270 mm (10.63 in.) deep strengthened beams and the 350  
34 mm (13.78 in.) deep strengthened beams did not show any significant difference in capacity.

1 During testing, it was clear that pre-existing cracks were interacting with subsequent crack  
2 formation yet interestingly this interaction did not seem to impact greatly on the peak load at  
3 failure. As will be explained later in this paper, the strengthened beams failed due to the  
4 debonding of the CFRP sheets. Such debonding failures could conceal any possible load  
5 effects that may have affected the shear force capacity at a further loading stage. This  
6 possibility may be further investigated by preventing debonding at a fairly early stage. This  
7 can be achieved either by fully wrapping the beam or, more practically, by using fasteners to  
8 secure the CFRP sheets and so exploit its tensile strength more effectively.

9 The CFRP contribution of the strengthened beams was clearly affected by the change in beam  
10 depth. It increased with increasing depth from 14.5 kN (3.26 kips) to 28 kN (6.30 kips) in the  
11 strengthened beams subjected to LP1 and from 8.5 kN (1.91 kips) to 26.5 kN (5.96 kips) in  
12 the strengthened beams subjected to LP2. These results suggest that the bonded fabric system  
13 is more effective when used on the “deeper” 350 mm (13.78 in.) beams. In the “shallower”  
14 270 mm (10.63 in.) deep specimens, the fabric strengthening was not fully effective since  
15 only a fairly short bonded length is available for force transfer. Another explanation could be  
16 that the “deeper” beams had more CFRP area bridging a shear crack compared to the  
17 “shallower” beams.

18

### 19 **Shear force-deflection relationship**

20 The shear force-deflection curves for the specimens considered in this investigation are  
21 presented in **Fig. 4**. Except for F/295/LP1/3.3 which failed in flexure, all specimens  
22 experienced a drop in load at peak shear force which is a characteristic of brittle (shear)  
23 failure. The unstrengthened specimens were more brittle compared to the corresponding  
24 strengthened specimens. The deflection ratio between the strengthened beams that failed in  
25 shear and the corresponding unstrengthened beams, however, is of the same order of  
26 magnitude, approximately 1.22.

27 In the initial loading stage (up to 70% of the unstrengthened capacity), the strengthened  
28 beams, except F/215/LP2/4.6 as it was initially loaded at a shorter shear span, behaved  
29 similarly to the corresponding unstrengthened specimens.

30 In the final loading stage, all the strengthened beams attained slightly higher stiffness, which  
31 deteriorated gradually with increased loading due to cracking until failure occurred.  
32 Specimens U/295/LP2/4.5 and F/295/LP2/4.5 show stiffer shear force-deflection  
33 relationships as they had shorter lengths.

1 Specimen F/295/LP1/3.3 had the same geometrical dimensions as the other 350 mm (13.78  
2 in.) deep specimens. However, its longitudinal steel ratio was 27% less. That is why, after the  
3 initial flexural cracking of the concrete at a shear force of about 20 kN (4.5 kips), this beam  
4 experienced more deflection at a given shear force compared to U/295/LP1/4.5 and  
5 F/295/LP1/4.5. This difference in deflection at the end of the pre-cracking process was in  
6 excess of 2mm (0.08 in.). Except for the extra deflection, at reloading the behavior of  
7 F/295/LP1/3.3 was similar to that of F/295/LP1/4.5 up to a shear force of 122.5 kN (27.54  
8 kips). At that load level, the beam developed ductile behavior as illustrated by the  
9 approximately 10 mm (0.39 in.) long yield plateau seen in **Fig. 4** and then failed in flexure.

### 11 **Failure mode**

12 The two unstrengthened beams failed in shear as shown in **Fig. 5**. U/295/LP0/4.5 failed due  
13 to an inclined crack that ran from the support to the load point. This inclined crack followed a  
14 path at an angle of approximately  $24^\circ$  in the web and a much shallower path in the flange.

15 Specimen U/295/LP2/4.5 failed due to an inclined crack that penetrated the flange and  
16 propagated towards the load pad. This was accompanied by the excessive opening of one of  
17 the inclined cracks in the web as shown in **Fig. 5**. Of importance is that the inclined shear  
18 crack that formed in the first stage of loading remained stable and did not contribute to the  
19 failure mechanism. This may explain why load case LP2 had little effect on the shear  
20 carrying capacity.

21 Specimens F/295/LP1/4.5 and F/295/LP2/4.5 failed due to an inclined crack that extended  
22 into the flange and ran to the load pad. This was preceded by the debonding of the CFRP  
23 sheets located between the splitting zones shown in **Fig. 6** and the load pads. The fabric  
24 splitting was caused by a set of vertical cracks that formed initially in the flange and extended  
25 downward to the web. The formation of such cracks in the flange can be explained by strain  
26 compatibility between the flange and the web. With increased loading, the web portion  
27 between the support and the major shear crack attempts to rotate. However, the flange  
28 restrains its movement. Consequently, horizontal tensile strains and stresses develop in the  
29 top part of the flange. Eventually, the tensile stresses exceed the tensile strength of the  
30 concrete and vertical cracks form. Hence, the fabric splitting close to the support region of  
31 the beam may be prevented by applying a layer of the unidirectional CFRP sheets parallel to  
32 the longitudinal axis of the beam.

1 Specimen F/215/LP2/4.6, which was tested before F/215/LP1/4.6, is pictured at failure in  
2 **Fig. 7**. Initially, the fabrics started to peel off at the web-flange interface closer to the support.  
3 The beam failed due to peeling off of the fabrics and concrete failure in the end region of the  
4 beam before the inclined cracks could reach the load pad. However, the penetration of the  
5 inclined cracks well into the flange and their progress toward the load pad were signs that  
6 shear failure was imminent. It is possible that the reduced support area in this specimen due  
7 to chamfering and the relatively short overhang might have led to concrete failure in the end  
8 region of the beam.

9 When the support area was not chamfered and the overhang length was increased in specimen  
10 F/215/LP1/4.6, the beam failed in shear as shown in **Fig. 7**. The fabrics started to peel off in a  
11 similar way to that of F/215/LP2/4.6 and the inclined cracks continued to propagate towards  
12 the load pad and backwards above the support and into the overhang until, eventually, they  
13 led to beam failure. This was accompanied by separation between concrete and fabrics as can  
14 also be seen in **Fig. 7**.

15 Specimen F/295/LP1/3.3 failed in flexure due to the crushing of the concrete in the  
16 compression zone at the middle of the beam as shown in **Fig. 8**. This result is important as it  
17 shows that the externally bonded CFRP sheets can change the mode of failure from a brittle  
18 shear failure to a ductile flexural failure. The CFRP composites in the two shear spans of  
19 F/295/LP1/3.3 were still intact and bonded to the beam web at failure.

20 It was not possible to measure the width of shear cracks in the strengthened specimens as  
21 these cracks were covered by the CFRP sheets. Nevertheless, It was expected that very  
22 limited size effects, if any, existed due to the limited increase in beam depth from 270 mm  
23 (10.63 in.) to 350 mm (13.78 in.).

24

### 25 **Strain in the steel shear reinforcement**

26 This section reports on the strain in the transverse steel reinforcement in the shear spans  
27 where failure occurred. **Fig. 3** shows the positions of the strain gauges on the transverse steel  
28 reinforcement. For the purpose of interpreting results, the shear links are categorized into  
29 “outer links” (TR1), “middle links” (TR2 and TR3 in the 350 mm [13.78 in.] deep specimens,  
30 and TR2 in the 270 mm [10.63 in.] deep specimens) and “inner links” (TR4 in the 350 mm  
31 [13.78 in.] deep specimens and TR3 in the 270 mm [10.63 in.] deep specimens).  
32 Unfortunately, some strain gauges failed during testing and their results were discarded.

33 The outer and middle shear links in the unstrengthened beams started to function only after a  
34 shear force of between 30 kN (6.74 kips) and 45 kN (10.12 kips) (see **Fig. 9**). Thereafter, the

1 strain in the stirrups increased significantly with increasing load. Most of the shear links in  
2 this group attained their yield strain after a shear force of approximately 90 kN (20.23 kips).  
3 This was expected since these links were crossed by the major shear cracks.  
4 The outer and middle shear links in the strengthened beams experienced five phases during  
5 loading. In the initial phase, which is bounded on the upper end by a shear force between 35  
6 kN (7.87 kips) and 45 kN (10.12 kips), the contribution of the shear links to the resistance  
7 was negligible. In the second phase, which included loading to 70% of the unstrengthened  
8 shear capacity, the shear links started to develop strain due to the initiation and propagation  
9 of inclined cracks. In the third phase, unloading to 40% of the unstrengthened shear capacity  
10 reduced the strain in the outer and middle shear links. The fourth phase is marked by the  
11 addition of the CFRP sheets and the stiffer response shown by the transverse steel  
12 reinforcement on further reloading. The transverse steel strain showed limited increases with  
13 increasing load until, in the final stage, yielding was achieved in most cases. The transverse  
14 steel reinforcement that yielded is easily identified by the plateaus featured in **Fig. 9**.  
15 **Fig. 9** also shows that the inner links carried the least amount of strain in all test specimens.  
16 The strains in this group of transverse reinforcement developed at a relatively low rate even  
17 after the formation of shear cracks. This is mainly because the beam region close to the load  
18 pad, where the inner links were located, did not experience significant inclined cracking.

19

### 20 **Strain in the CFRP sheets**

21 The shear force-strain curves for the externally bonded CFRP sheets in the shear spans where  
22 failure occurred are shown in **Fig. 9**. The positions of the strain gauges are given in **Fig. 3**.  
23 The fabrics are categorized into “outer fabrics” (CF1), “middle fabrics” (CF2 and CF3 in the  
24 350 mm [13.78 in.] deep specimens, and CF2 in the 270 mm [10.63 in.] deep specimens) and  
25 “inner fabrics” (CF4 in the 350 mm [13.78 in.] deep specimens and CF3 in the 270 mm  
26 [10.63 in.] deep specimens). Some strain gauges failed during testing and their results were  
27 discarded due to the erroneous data they provided.

28 The curves feature two phases. In the first phase, the fabrics started to resist the further  
29 opening of existing shear cracks at the inception of the final reloading stage. They continued  
30 to develop tensile strain with increased load up to approximately the peak loads. In the  
31 second stage, the fabrics started to debond and finally peeled off. Debonding is indicated by  
32 the reversing of the shear force-strain curves.

33 In a given beam, the middle fabrics – represented by CF3 in the 350 mm (13.78 in.) deep  
34 specimens and CF2 in the 270 mm (10.63 in.) deep specimens – developed the highest strain.

1 The sheets bonded to the 350 mm (13.78 in.) deep specimens developed higher strains  
2 compared to those bonded to the 270 mm (10.63 in.) deep specimens. This increase in the  
3 effectiveness of the fabrics can be explained by the increase in bond length. This result  
4 highlights the fact that the deeper the section, the higher the potential of the sheets to  
5 experience strain and hence provide shear enhancement.

## 6 7 **COMPARISON OF EXPERIMENTAL RESULTS WITH PREDICTIONS** 8 **OF SHEAR STRENGTHENING DESIGN GUIDELINES**

9 Design guidelines for externally bonded FRP shear reinforcement have been developed in the  
10 UK and elsewhere. In the UK, the Concrete Society Technical Report 55<sup>5</sup> (TR 55) is the first  
11 – and currently the sole – standard document to give guidance on the design of externally  
12 bonded FRP shear reinforcement. The design procedure adopted by TR 55<sup>5</sup> is based upon that  
13 proposed by Denton et al.<sup>15</sup> and assumes that the ultimate shear capacity of an FRP  
14 strengthened beam can be expressed as the sum of the shear forces carried by the concrete,  
15 the internal steel shear reinforcement and the external FRP shear reinforcement. Similarly,  
16 the ACI 440.2R-08<sup>4</sup> shear strengthening design model, based on work by Khalifa et al.<sup>16</sup>, and  
17 *fib* Bulletin 14<sup>6</sup> shear strengthening design guidelines, based on work by Triantafillou and  
18 Antonopoulos<sup>17</sup>, use the same approach as TR55<sup>5</sup>, assuming that the shear capacity of a  
19 strengthened RC beam can be expressed as the sum of the concrete, steel and FRP  
20 contributions. Further, the FRP contribution in the three aforementioned design guidelines is  
21 determined by adopting the truss analogy and assuming the inclination angle of the shear  
22 cracks to be 45°. The main difference among the three models is in the method of evaluating  
23 the effective strain in the FRP reinforcement.

24 A database of eight experimental results against which to compare the predictions of ACI  
25 440.2R-08<sup>4</sup>, TR55<sup>5</sup> and *fib* Bulletin 14<sup>6</sup> has been assembled. The database beams had T-  
26 shaped cross-sections, internal steel shear reinforcement, and shear span to effective depth  
27 ratios greater than or equal to 2.5. Although the design guidelines should be validated with a  
28 larger database, there have not been so many tests on RC Beams that meet the above criteria.  
29 RC beams that do not meet the above criteria are deemed to lie beyond the scope of this study  
30 and hence are not included in the database.

31 Three of the database beams are the fabric-strengthened beams F/295/LP1/4.5, F/295/LP2/4.5,  
32 and F/215/LP1/4.6 detailed in this study. The other five beams are SB-S1-2L-175 and SB-S1-  
33 0.5L-350 tested by Bousselham and Chaallal<sup>7,8</sup>, Specimen No. 2 tested by Sato et al.<sup>18</sup>, and  
34 T4S2-C45 and T6S4-C90 tested by Deniaud and Cheng<sup>19,20</sup>. All beams included in the

1 database, except those tested by Deniaud and Cheng<sup>19,20</sup>, were strengthened with continuous  
2 U-shaped externally bonded CFRP shear reinforcement. The externally bonded shear  
3 reinforcement in the beams tested by Deniaud and Cheng<sup>19,20</sup> consisted of CFRP U-strips  
4 spaced 100 mm (3.94 in.) c/c. All beams included in the database failed in shear due to the  
5 peeling off of the CFRP reinforcement.

6 **Table 5** compares the contributions of the externally bonded CFRP system predicted by the  
7 ACI 440.2R-08<sup>4</sup>, TR55<sup>5</sup> and *fib* Bulletin 14<sup>6</sup> design guidelines with the experimental results  
8 from the literature and the testing described in this paper. All safety factors are set equal to  
9 1.00 for the purpose of the comparison except for the ACI 440.2R-08<sup>4</sup> FRP strength reduction  
10 factor,  $\psi_f$ , which is set equal to 0.85 as it is an integral part of the nominal shear capacity  
11 expression. The experimental contributions of the CFRP sheets were calculated by  
12 subtracting the experimental unstrengthened shear capacity from the experimental  
13 strengthened shear capacity for each beam. It should be noted that some of the strengthened  
14 beams reported in this paper had slightly higher concrete compressive strength than the  
15 corresponding unstrengthened beams. However, further analyses carried out by the authors  
16 (not reported in this paper) showed that this slight difference in the concrete compressive  
17 strength had little significant effect on the predicted FRP contribution.

18 The total predicted shear force has not been compared to the total experimental shear force  
19 because such a comparison can lead to erroneous conclusions. Such a comparison requires  
20 the use of conventional design codes such as the Eurocode 2<sup>21</sup> (EC 2) to calculate the  
21 concrete and steel contributions to the total shear force capacity. Such codes often  
22 underestimate the concrete and steel contributions to the total shear force because they  
23 assume that only the web of the beam is effective when calculating the shear force capacity of  
24 a T-beam. For example, the total predicted shear force capacity of F/215/LP1/4.6 using the  
25 EC 2<sup>21</sup> and the TR 55<sup>5</sup> design equations is 94.1 kN (21.15 kips). As the total experimental  
26 shear capacity of F/215/LP1/4.6 is 102.5 kN (23.04 kips), this would lead to the conclusion  
27 that the design model of the TR 55<sup>5</sup> which overestimates the FRP contribution to the shear  
28 force capacity of F/215/LP1/4.6 by a factor of 2.08, is safe. Hence, while comparing the total  
29 experimental shear force capacity to the total predicted shear force capacity could result in a  
30 conservative prediction; such a comparison may lead to the erroneous conclusion that an  
31 over-conservative CFRP design model is safe.

32 The ACI 440.2R-08<sup>4</sup> design model is statistically the best model among the three design  
33 models investigated. However, the ACI 440.2R-08<sup>4</sup> design model has a mean predicted to  
34 experimental ratio of 1.41 and a standard deviation of 0.53. This is probably due to the fact

1 that the bond model used in the ACI 440.2R-08<sup>4</sup> design model is based on limited  
2 experimental data.

3 The TR 55<sup>5</sup> predictions overestimated the contributions of the externally bonded CFRP sheets  
4 to the shear force capacity with a mean predicted to experimental ratio of 1.64 and a standard  
5 deviation of 0.62. The inaccuracy of the TR 55<sup>5</sup> predictions stems from the inaccuracy of its  
6 effective strain model. TR55<sup>5</sup> predicts that the effective strain in the CFRP sheets of  
7 F/295/LP1/4.5, F/295/LP2/4.5 and F/215/LP1/4.5 is approximately 2560 micro-strain, 2650  
8 micro-strain and 2810 micro-strain respectively. The experimentally measured CFRP strain  
9 for these beams varied between 125 micro-strain and 1200 micro-strain (see **Fig. 9**).

10 The *fib* Bulletin 14<sup>6</sup> design model is statistically the worst model among the three design  
11 models investigated. It has a mean predicted to experimental ratio of 2.52 and a standard  
12 deviation of 0.76. The deficiency of the model is probably due to the fact that the equations  
13 for the effective FRP strain were obtained by regression analysis with limited experimental  
14 data. Hence, the effective FRP strain equations do not consider the bond mechanism which  
15 affects the mode of failure.

16

17

## SUMMARY AND CONCLUSIONS

18 This study investigates the structural behavior of precracked RC T-beams strengthened in  
19 shear with externally bonded CFRP sheets. The influence of load history, effective depth of  
20 the beam and longitudinal steel ratio on the strengthened behavior was studied. The  
21 predictions of three international shear strengthening design guidelines were compared with  
22 experimental results. Based on the results of this study, the following conclusions are drawn:

23 1. All strengthened specimens exhibited greater capacities than equivalent  
24 unstrengthened control beams, with capacity enhancements ranging from 9.7% to  
25 26.2%, confirming the potential effectiveness of the CFRP sheets.

26 2. The two loading patterns investigated, LP1 and LP2, did not generally seem to have a  
27 significant effect on the shear capacity of the strengthened beams. During testing it  
28 was clear that pre-existing cracks were interacting with subsequent crack formations  
29 yet this interaction did not seem to impact greatly on the peak load at failure.

30 3. The increase in beam depth positively affected the contribution of the CFRP sheets to  
31 the shear force capacity through providing additional bond length to better exploit the  
32 sheets' tensile strength.

33 4. The decrease in the longitudinal reinforcement ratio from 4.5% to 3.3% changed the  
34 mode of failure from brittle shear failure to ductile flexural failure.



- 1 6. *fib* Task Group 9.3, “Bulletin 14: Externally Bonded FRP Reinforcement for RC  
2 Structures,” International Federation for Structural Concrete (*fib*), Lausanne, Switzerland,  
3 2001, 138 pp.
- 4 7. Bousselham, A., and Chaallal, O., “Effect of Transverse Steel and Shear Span on the  
5 Performance of RC Beams Strengthened in Shear with CFRP,” *Composites Part B:  
6 Engineering*, Elsevier, The Netherlands, V. 37, No. 1, 2006, pp. 37-46.
- 7 8. Bousselham, A., and Chaallal, O., “Behaviour of Reinforced Concrete T-Beams  
8 Strengthened in Shear with Carbon Fiber-Reinforced Polymer – An Experimental Study,”  
9 *ACI Structural Journal*, V. 103, No. 3, 2006, pp. 339-347.
- 10 9. Khalifa, A., and Nanni, A., “Rehabilitation of Rectangular Simply Supported RC Beams  
11 with Shear Deficiencies Using CFRP Composites,” *Construction and Building Materials*,  
12 Elsevier, The Netherlands, V. 16, No. 3, 2002, pp. 135-146.
- 13 10. Pellegrino, C., and Modena, C., “Fiber Reinforced Polymer Shear Strengthening of  
14 Reinforced Concrete Beams with Transverse Steel Reinforcement,” *ASCE Journal of  
15 Composites for Construction*, V. 6, No. 2, 2002, pp. 104-111.
- 16 11. Chaallal, O., Shahawy, M., and Hassan, M., “Performance of Reinforced Concrete T-  
17 Girders Strengthened in Shear with Carbon Fiber-Reinforced Polymer Fabrics,” *ACI  
18 Structural Journal*, V. 99, No. 3, 2002, pp. 335-343.
- 19 12. Sika Limited, “SikaWrap-230C Product Data Sheet,” United Kingdom, 2005, 4pp.
- 20 13. Sika Limited, “Sikadur-330 Product Data Sheet,” United Kingdom, 2005, 6pp.
- 21 14. Hoult, N. A., and Lees, J. M., “Efficient CFRP Strap Configurations for the Shear  
22 Strengthening of Reinforced Concrete T-Beams,” *ASCE Journal of Composites for  
23 Construction*, V. 13, No. 1, 2009, pp. 45-52.
- 24 15. Denton, S. R., Shave, J. D., and Porter, A. D., “Shear Strengthening of Reinforced  
25 Concrete Structures Using FRP Composites,” *Proceedings of the 2<sup>nd</sup> International  
26 Conference on Advanced Polymer Composites for Structural Applications in Construction  
27 (ACIC 2004)*, Woodhead Publishing Ltd., United Kingdom, 2004, pp. 134-143.
- 28 16. Khalifa, A., Gold, W. J., Nanni, A., and Aziz, A. M. I., “Contribution of Externally  
29 Bonded FRP to Shear Capacity of RC Flexural Members,” *ASCE Journal of Composites for  
30 Construction*, V. 2, No. 4, 1998, pp. 195-202.
- 31 17. Triantafillou, T. C., and Antonopoulos, C. P., “Design of Concrete Flexural Members  
32 Strengthened in Shear with FRP,” *ASCE Journal of Composites for Construction*, V. 4, No. 4,  
33 2000, pp. 198-205.

- 1 18. Sato, Y., Ueda, T., Kakuta, Y., and Ono, S., “Ultimate Shear Capacity of Reinforced  
2 Concrete Beams with Carbon Fiber Sheet,” *Proceedings of the 3<sup>rd</sup> International Symposium*  
3 *on Non-Metallic (FRP) Reinforcement for Concrete Structures*, Japan Concrete Institute,  
4 Japan, V. 1, 1997, pp. 499-506.
- 5 19. Deniaud, C., and Cheng, J. J. R., “Reinforced Concrete T-Beams Strengthened in Shear  
6 with Fiber Reinforced Polymer Sheets,” *ASCE Journal of Composites for Construction*, V. 7,  
7 No. 4, 2003, pp. 302-310.
- 8 20. Deniaud, C., and Cheng, J. J. R., “Shear Behavior of Reinforced Concrete T-Beams with  
9 Externally Bonded Fiber-Reinforced Polymer Sheets,” *ACI Structural Journal*, V. 98, No. 3,  
10 2001, pp. 386-394.
- 11 21. British Standards Institution, “Eurocode 2: Design of Concrete Structures – Part 1-1:  
12 General Rules and Rules for Buildings,” London, England, 2004, 225pp.

13  
14  
15  
16  
17  
18  
19  
20  
21  
22  
23  
24  
25  
26  
27  
28  
29  
30  
31  
32  
33  
34

1

**Table 1–Summary of test specimens**

Specimen	$f_{cu}$ , MPa (ksi)	$a$ , mm (in.)	$d$ , mm (in.)	$A_s$ , mm <sup>2</sup> (in. <sup>2</sup> )
U/295/LP 0/4.5	24 (3.48)	1125 (44.29)	295 (11.61)	1383 (2.14)
U/295/LP 2/4.5	28 (4.06)	1125 (44.29)	295 (11.61)	1383 (2.14)
F/295/LP 1/4.5	24 (3.48)	1125 (44.29)	295 (11.61)	1383 (2.14)
F/295/LP 2/4.5	27 (3.92)	1125 (44.29)	295 (11.61)	1383 (2.14)
F/295/LP 1/3.3	28 (4.06)	1125 (44.29)	295 (11.61)	1030 (1.60)
F/215/LP 1/4.6	32 (4.64)	820 (32.28)	215 (8.46)	1030 (1.60)
F/215/LP 2/4.6	25 (3.63)	820 (32.28)	215 (8.46)	1030 (1.60)

2

3

**Table 2–Steel reinforcement properties**

Bar diameter, mm (in.)	Yield strength, MPa (ksi)	Yield strain	Ultimate strength, MPa (ksi)
6 (0.24)	580 (84.12)*	0.0050*	586 (84.99)
8 (0.31)	520 (75.42)	0.0028	594 (86.15)
16 (0.63)	500 (72.52)	0.0032	593 (86.01)
20 (0.79)	580 (84.12)	0.0038	680 (98.63)
25 (0.98)	440 (63.82)*	0.0044*	540 (78.32)

4

5

\* Using the 0.2% offset method.

6

7

**Table 3–CFRP sheets and adhesive properties**

Material	Tensile strength, MPa (ksi)	Ultimate strain	Elastic modulus, MPa (ksi)
CFRP sheets*	4300 (623.66)	0.0180	238000 (34519)
Epoxy resin	30 (4.35)	0.0090	4500 (653)
Composite material**	350 (50.76)	0.0125	28000 (4061)

8

9

\* Nominal thickness per layer = 0.131 mm (0.0052 in.).

10

\*\* Nominal thickness per layer = 1 mm (0.0394 in.).

1

**Table 4–Experimental results**

Specimen	Unstrengthened shear capacity, kN (kips)	Shear force at failure, kN (kips)	Gain in shear strength, kN (kips)	Gain in shear strength, %
U/295/LP 0/4.5	107.0 (24.05)	107.0 (24.05)	0 (0)	0
U/295/LP 2/4.5	107.0* (24.05)	116.0 (26.08)	9 (2.03)	8.4
F/295/LP 1/4.5	107.0 (24.05)	135.0 (30.35)	28.0 (6.30)	26.2
F/295/LP 2/4.5	107.0 (24.05)	133.5 (30.01)	26.5 (5.96)	24.8
F/295/LP 1/3.3	107.0 (24.05)	122.5 (27.54)	15.5 (3.49)	14.5
F/215/LP 1/4.6	88.0** (19.78)	102.5 (23.04)	14.5 (3.26)	16.5
F/215/LP 2/4.6	88.0** (19.78)	96.5 (21.69)	8.5 (1.91)	9.7

2

3

\* For purpose of comparison with U/295/LP0/4.5.

4

\*\* Based on the control beam, tested by Hoult and Lees<sup>14</sup>, which is nominally identical to F/215/LP1/4.6 and F/215/LP2/4.6.

5

6

**Table 5–Experimental versus predicted shear resistance due to FRPs**

Specimen	Experimental, kN (kips)	ACI 440.2R -08 <sup>4</sup> , kN (kips)	TR55 <sup>5</sup> , kN (kips)	<i>fib</i> Bulletin 14 <sup>6</sup> , kN (kips)
F/295/LP1 /4.5	28.0 (6.30)	51.4 (11.56)	63.1 (14.19)	70.1 (15.76)
F/295/LP2 /4.5	26.5 (5.96)	56.7 (12.74)	66.7 (14.99)	74.1 (16.66)
F/215/LP1 /4.6	14.5 (3.26)	31.6 (7.11)	30.1 (6.77)	57.5 (12.93)
SB-S1-2L-175 <sup>7</sup>	12.2 (2.74)	14.9 (3.34)	21.8 (4.90)	26.6 (5.98)
SB-S1-0.5L-350 <sup>8</sup>	19.2 (4.32)	23.5 (5.30)	23.0 (5.17)	49.0 (11.02)
Specimen No. 2 <sup>18</sup>	24.0 (5.40)	21.8 (4.90)	23.9 (5.37)	50.2 (11.29)
T4S2-C45 <sup>19</sup>	17.8 (4.00)	19.2 (4.32)	30.2 (6.79)	52.2 (11.74)
T6S4-C90 <sup>20</sup>	85.3 (19.18)	61.0 (13.72)	50.2 (11.29)	95.8 (21.54)

7

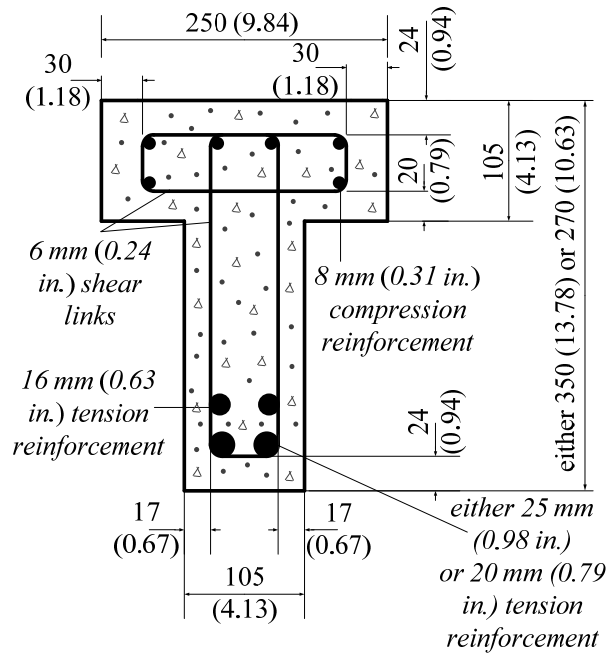


**Fig. 1– Cross-sections details – dimensions in mm (in.).**

1  
2  
3  
4

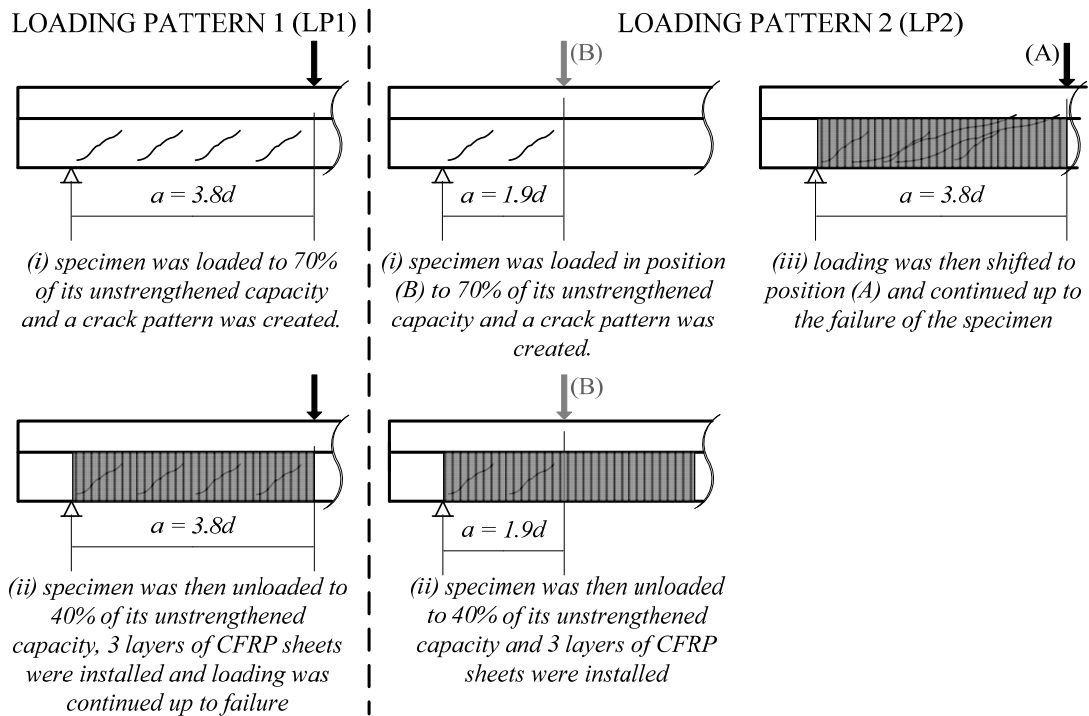


**Fig. 2–Loading patterns.**

5  
6  
7

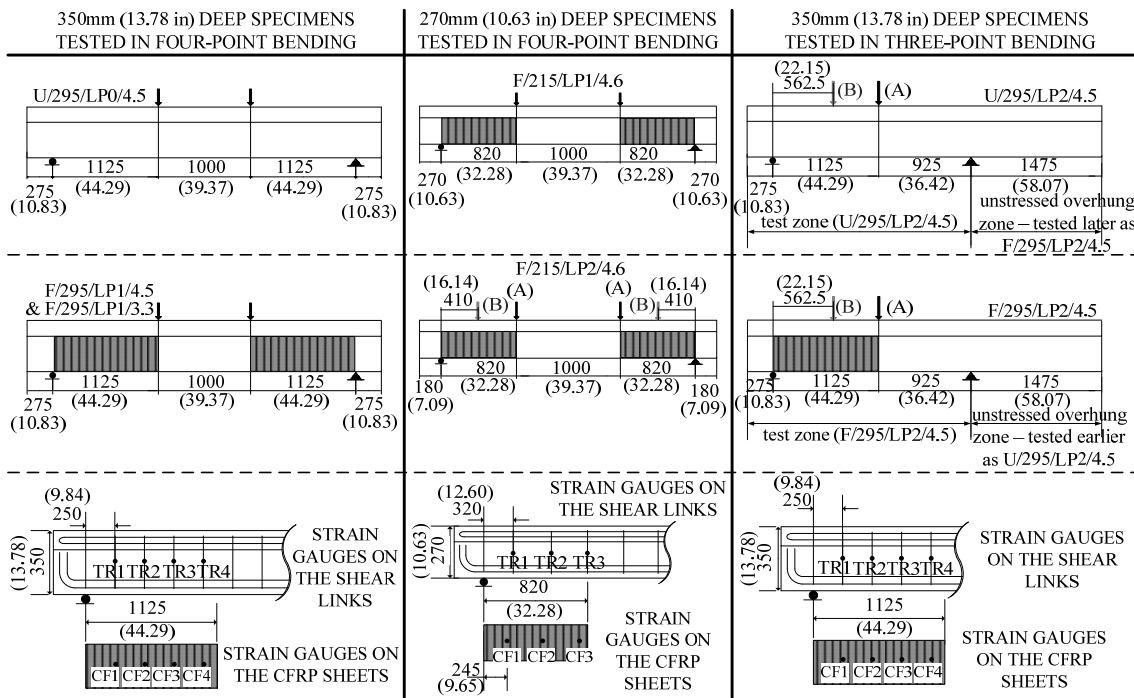


Fig. 3– Details of test specimens – dimensions in mm (in.).

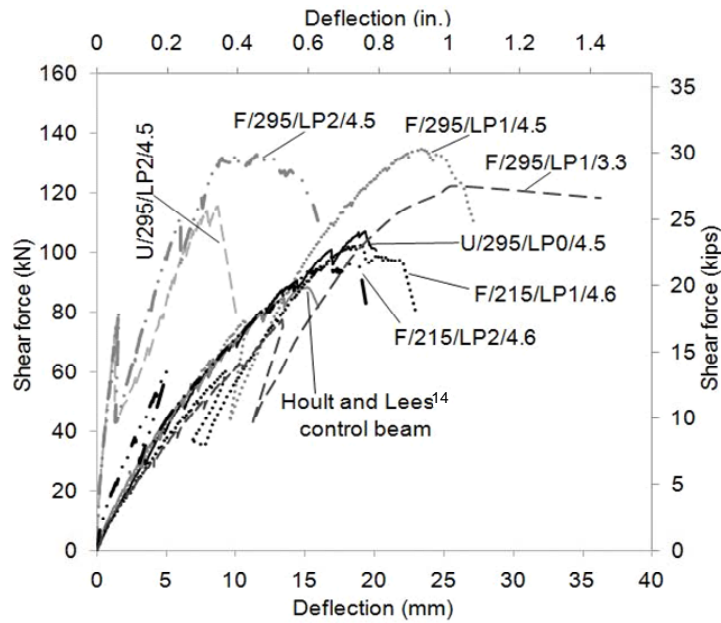
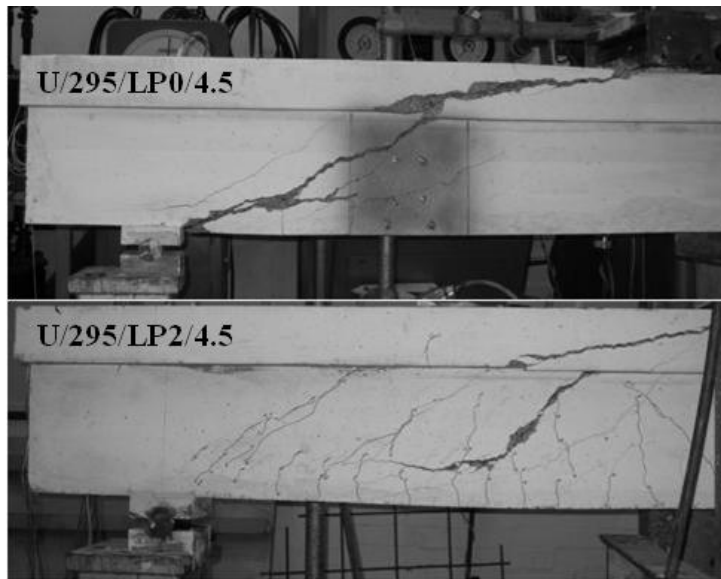
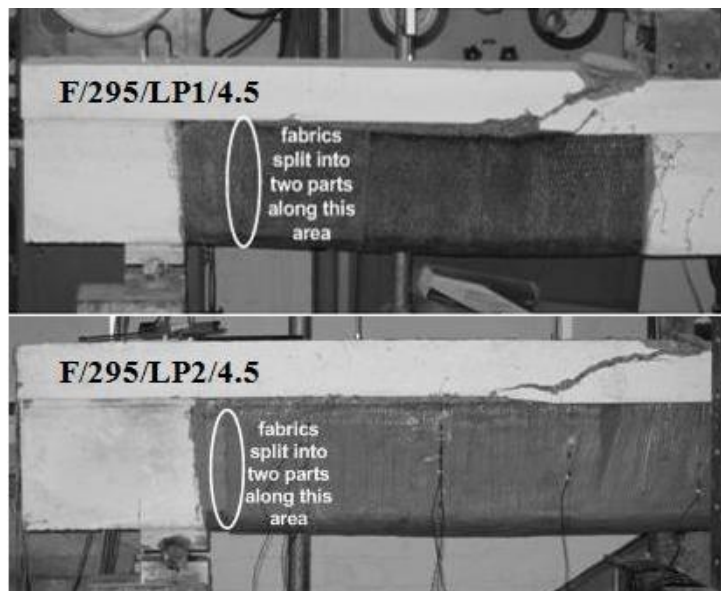


Fig. 4– Shear force-deflection curves.



**Fig. 5–Unstrengthened specimens at failure.**



**Fig. 6–F/295/LP1/4.5 and F/295/LP2/4.5 at failure.**



**Fig. 7–F/215/LP1/4.6 and F/215/LP2/4.6 at failure.**



**Fig. 8–Flexural failure of F/295/LP1/3.3.**

1  
2  
3

4  
5  
6  
7  
8  
9  
10  
11

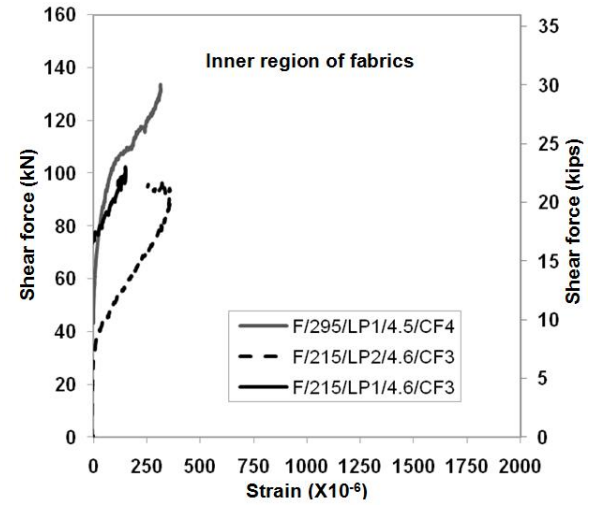
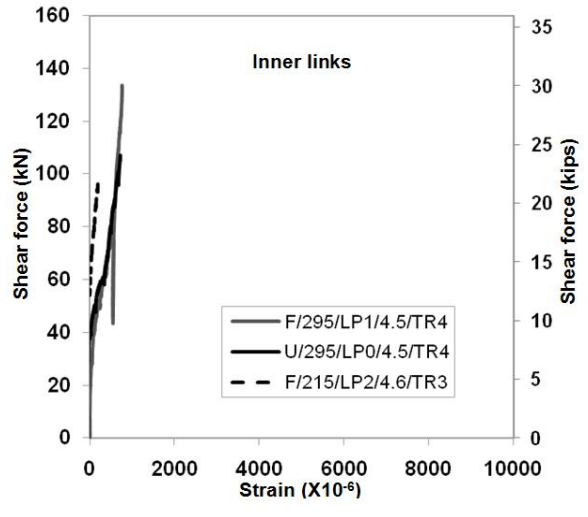
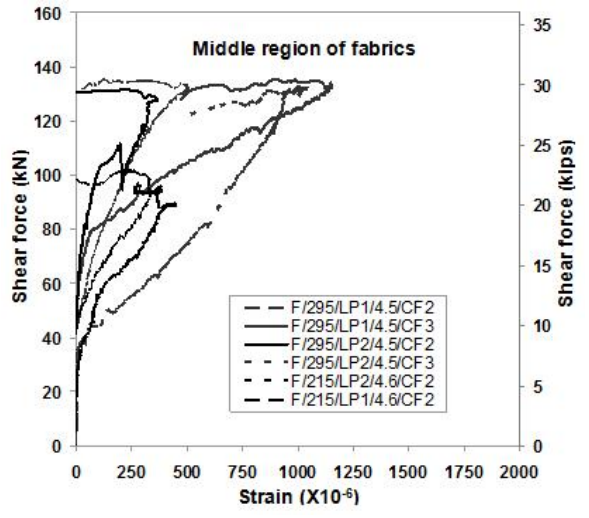
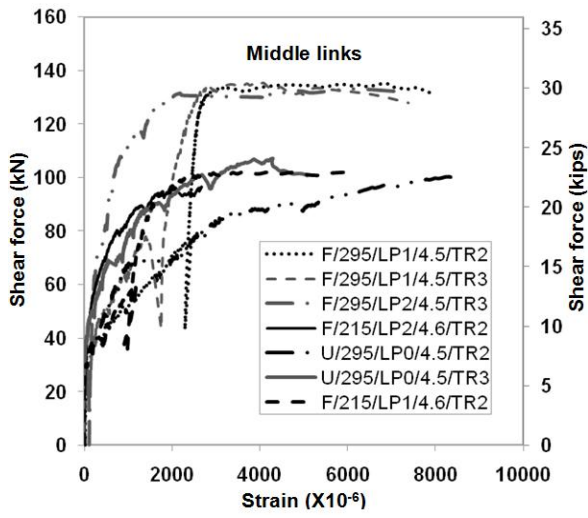
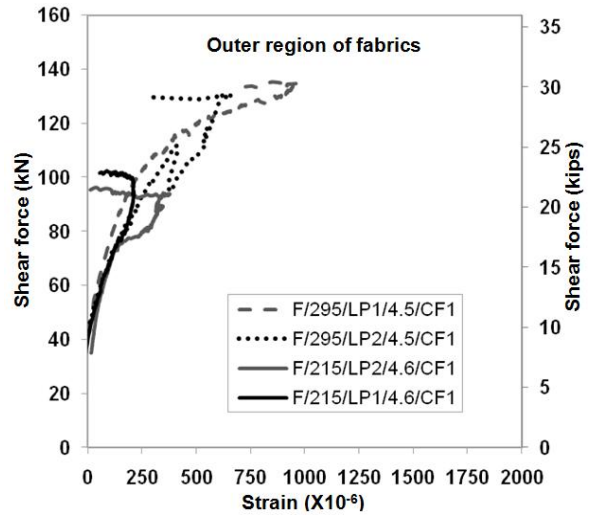
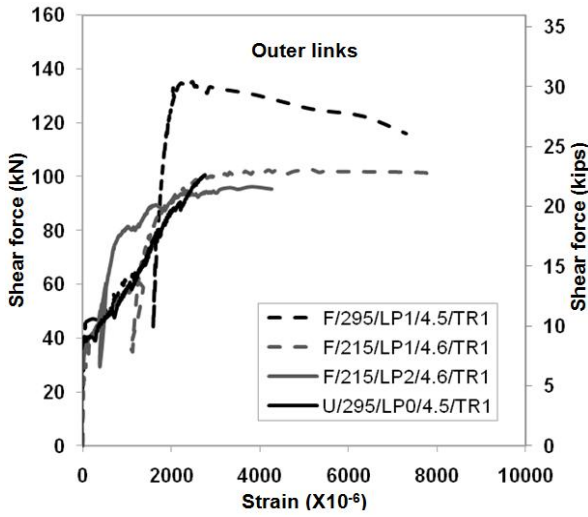


Fig. 9–Shear force versus strain in the internal and external shear reinforcement.